Journal of Molecular Structure 1198 (2019) 126899

Contents lists available at ScienceDirect

Journal of Molecular Structure

journal homepage: http://www.elsevier.com/locate/molstruc

New thiazoldinone substituted 2,6-diarypiperidin-4-one: Synthesis, crystal structure, spectral characterization, binding mode with calf thymus DNA

P. Sangeetha [a], C. Sankar [b], K. Tharini [c, *]

[a] Department of Chemistry, Rajah Serfoji Government College, Thanjavur, 613 005, India
[b] Department of Chemistry, SRM-TRP Engineering College, Tiruchirappalli, 626 126, India
[c] Department of Chemistry, Govt. Arts College, Tiruchirappalli, 620 022, India

ARTICLE INFO

Article history:
Received 25 February 2019
Received in revised form
31 July 2019
Accepted 3 August 2019
Available online 8 August 2019

Keywords:
Piperdin-4-ones
Thiazolidinone
NMR
Conformation
DNA binding
Single crystal

ABSTRACT

A series of 2,6-diarylpiperidin-4-ylidene thiazolidin-4-one derivatives (**15**–**21**) were efficiently synthesized using a green and recyclable catalyst Amberlit IR-120H resin under microwave irradiation. All the compounds were characterized by elemental analysis, FT-IR, ^{1}H, ^{13}C NMR spectra. The conformation of the compound was unambiguously assigned by 2D NMR spectral analysis. Single crystal X-ray diffraction recorded for compound **21** and the data indicate that the compound crystallized in triclinic system with space group $P\bar{1}$. The observed chemical shifts and coupling constants suggested that the piperidone ring (**15**–**21**) adopts in chair conformation with equatorial orientations of the aryl groups. In solid state the configuration about C=N double bond is *syn* to C-5 carbon. All the compounds were screened for their *in vitro* antibacterial and antimycobacterial activities. Among the tested, compounds **17** and **18**, were found to be potent inhibition with MIC values in the range of 0.2–0.8 μg/mL.

The interactions of the compounds with calf thymus DNA were investigated by spectroscopic method and the results indicated that compounds bound to Deoxyribo Nucleic Acid (DNA) by groove binding mode.

1. Introduction

Tuberculosis (TB) continues to be a serious and potentially fatal infection with a worldwide distribution. The World Health Organization (WHO) reported TB is the ninth foremost cause of death worldwide and leading cause from a single infectious agent [1]. The high mortality rate of TB has even beaten the number of deaths caused by human immunodeficiency virus [1]. Worldwide, the mortality rate due to TB has dropped by 3% per year and new TB cases have decreased only about 2% per year [2]. Furthermore, according to an estimate one-third of the world's population is infected with a latent form of TB [3]. The appearance of multidrug-resistant TB (MDR–TB) has given a huge challenge throughout the world in the fight against TB [4]. All the above facts reveal that there is a serious need for the development of new drugs with divergent unique structure and with a mechanism of action possibly different from that of existing drugs. These trends have emphasized the urgent need and challenge for the development of more effective, potent and broad spectrum antimicrobial novel drugs with good bioavailability to cure microbial infections [5]. In this context, the drug discovery has acquired a considerable interest in microbial target based synthesis of novel antimicrobial agents. Piperidone and their derivatives are considered as important scaffolds in medicinal field because it possesses a wide spectrum of biological activities such as antimicrobial [6], anti-cancer [7] and anti-proliferative [8] agents. Similarly thiazolidinone represents as an important and abundant class of nitrogen and sulphur containing heterocycle compound [9]. This class of compounds possess variety of biological activity, such as anti-tumor [10], antiviral [11], anti-mycobacterial [12], anticancer [13,14] and anticonvulsant [15] activities.

In recent years, several methods have been developed for the synthesis of thiazolidinone scaffolds. Unfortunately, some of these methods have relatively long reaction times, low yields, tedious workup procedures and co-occurrence of several side reactions.

* Corresponding author. Department of Chemistry, Govt. Arts College, Tiruchirappalli, 620 022, India.
E-mail address: tharinilenin@gmail.com (K. Tharini).

https://doi.org/10.1016/j.molstruc.2019.126899
0022-2860/

Thus, the introduction of green methods to overcome these limitations is still an important experimental challenge. Microwave assisted organic synthesis have become a new trend with many applications in synthesizing the organic molecules.

Heterogeneous catalysis has played an important role in various organic transformations. Heterogeneous solid acids like ion-exchange resins are superior to the conventional homogeneous acid catalysts due to their low cost, operational simplicity, low toxicity and environmental compatibility. Moreover, they can be easily recovered from reaction mixtures by simple filtration and can be reused with or without activation, making the process economically viable. Amberlite IR-120 acidic resin is one of the best examples of heterogeneous catalyst which is non-toxicity, reusability and easily separable solid acid catalysts, they have become progressively more important in organic synthesis in recent years [16].

In development of drugs for the tuberculosis, DNA is a one of the best target for development of specific drug candidates to TB by overcoming drug resistance. The DNA interacting molecules are usually bound to DNA non-covalently by three modes: intercalation, groove binding and static electronic interactions. Static electronic interactions refer to molecules that bind with the negatively charged DNA double helix externally through a non-specific interaction. In groove binding, the targeting molecules interact with DNA in the base edges of the major groove or minor groove, which had been discussed by many groups. The intercalation is another DNA binding mode that is closely related to the antitumor ability of many anticancer agents. Another thing need to understand while designing the drug in target specific by considering drug should not affect the normal physiological functions of the cells [17]. In this regard, the designing DNA binding drugs are leading approaches in the field of Tuberculosis therapy for the future.

Further, amino acid/peptide-based drugs have low toxicity, ample bioavailability and permeability, modest potency and good metabolic and pharmacokinetic properties [18]. Prompted by all these observations and with a further interest to develop more biologically active compounds, the present work encompasses the synthesis of novel amino acids conjugated thiazolidinone analogues as promising DNA binding and antitubercular agents.

2. Experimental

2.1. Purchasing materials

All chemicals and other solvents were either purchased as high purity and used without further purification or purified by standard procedure to their use. All the reactions were carried out using a conventional household microwave oven and reactions were monitored by TLC. Melting points were measured on open capillaries and are uncorrected. Elemental analyzes was performed on an Elementar Vario EL III CHNS analyzer.

2.2. Recording spectra

FT-IR spectra were recorded in an AVATAR-330 FT-IR Thermo-Nicholes spectrophotometer. ^{1}H NMR spectra was recorded at room temperature (298 K) on BRUKER DRX 500 NMR spectrometer operating at 500.03 MHz in DMSO-d_6.^{13}C NMR spectra was recorded in proton decoupled mode on BRUKER DRX 500 NMR spectrometer operating at 125.75 MHz. All NMR measurements were made on 5 mm NMR tubes. The solutions were prepared by dissolving about 10 mg of the compound in 0.5 mL of DMSO-d_6. UV−Visible study was carried out Shimadzu-2400 PC spectrometer. The fluorescence spectra were determined on Varian Cary Eclipse fluorescence spectrometer.

2.3. X-ray crystallography

Crystal was grown by slow evaporation technique using mixture of ethanol and ethyl acetate as solvent. Diffraction data were collected on a Bruker, 2004 APEX 2 diffractometer using graphite-monochromated MoKα radiation (K = 0.71073 Å) at 293 K with crystal size of 0.22 × 0.18 × 0.16 mm. The structure was solved by direct methods and successive Fourier difference syntheses (SHELXS-97) [19] and refined by full matrix least square procedure on F2 with anisotropic thermal parameters. All non-hydrogen atoms were refined (SHELXL-97) [20] and placed at chemically acceptable positions. The crystallographic data have been deposited with Cambridge Crystallographic Data Centre and the CCDC No. 1530656 for **21**.

2.4. UV-absorption spectra

Stock solution of compound (10 mM) was prepared in AR grade DMSO. Electronic absorption spectra was determined in the range of 280−350 nm by measuring the spectra of compound in 10% DMSO-10 mM at pH 7.4 by using Tris-HCl buffer mixture with increasing concentration of CT-DNA (from 0 to 60 μM). All the UV−visible spectra were recorded after equilibration of solution for 5 min. The buffer (10 mM Tris-HCl) was subtracted through base line correction. All the measurements were carried out at 25 °C with a scan speed of 960 nm min^{-1}.

2.5. Steady state fluorescence

The binding study was performed by fluorescence quenching titration experiments in a mixture of 10% DMSO-10 mM Tris-HCl buffer (pH 7.4). The fluorescence quenching was observed by titrating the fixed amount of compound (50 μM) with different concentration of CT-DNA (10−50 μM) bound to Ethidium Bromide (EB) (50 μM) at 25 °C. Each sample solution was shaken and allowed to stand for 5 min and then fluorescence spectra were recorded in the range of 500−650 nm with an excitation wavelength of 575 nm. The emission and excitation slit widths were adjusted to 10 nm each.

2.6. Thermal denaturation study

The compound was titrated with CT-DNA in the molar ratio of (1:1) and kept at 25 °C for 10 min. The absorbance of CT-DNA (50 μM) in 10% DMSO-10 mM Tris-HCl buffer mixture (pH 7.4) was measured at 320 nm in a temperature range from 30 °C to 100 °C. The absorbance of the compounds was subtracted from every curve, and the absorbance scale was normalized. The ΔT_m values were calculated by subtracting Tm of the free nucleic acid from Tm of the complex. Every reported ΔT_m value was the average of at least two measurements. The error of ΔT_m is ±0.5.

2.7. CD studies

CD spectra of CT-DNA (50 μM) were determined at room temperature by increasing the [compound]/[CT-DNA] ratio (r = 0, 1.0 and 2.0) in 10% DMSO-10 mM Tris-HCl buffer mixture (pH 7.4) in the range of 250−310 nm. The scan speed of 100 nm min^{-1} with a spectral bandwidth of 10 nm and its final CD spectrum was generated after averaging three scans and subtracting the buffer background.

2.8. Viscosity measurements

The Viscosity of the sample was done by using a viscosimeter

(SCHOT AVS 450) in thermostat at 25 °C. The CT-DNA concentration was kept at 50 μM and flow time was measured with a digital stop watch. The values of relative specific viscosity $(\eta/\eta^{\circ})^{1/3}$ where η° and η the specific viscosity contributions of DNA in the absence (η°) and in the presence of the drug (η°), were plotted against 1/R (R = [compound]/[DNA]).

2.9. Material synthesis

2.9.1. General procedure for synthesis of 5′-methyl-(3/5-alkyl-2r,6c-diarylpiperidin-4-ylidene)hydrazono)thiazolidin-4-one (**15**–**21**)

Thiosemicarbazone (1 mmol) and anhydrous sodium acetate (0.15 mmol) were dissolved in 50 mL of ethanol. The reaction mixture was then heated to reflux and a solution of equal amount of ethyl 2-bromopropionate (1 mmol) slowly added to the reaction mixture. After refluxing for about 4–5 h, the reaction mixture was cooled, excess solvent was removed under reduced pressure. The reaction mixture was poured into crushed ice. The separated solid was filtered off and purified by recrystallization using ethanol. For some cases, the target compounds could be purified by column chromatography using a mixture of chloroform – ethylacetate (8:2) as eluent.

2.9.2. General microwave method for synthesis of compound 5′-methyl-(3/5-alkyl-2r,6c-diarylpiperidin-4-ylidene)hydrazono) thiazolidin-4-one (**15**–**21**)

A mixture of 3/5-alkyl-2*r*,6*c*-diarylpiperidin-4-one, thiosemicarbazone and ethyl 2-bromopropionate (1:1 mol) were mixed thoroughly with a catalytic amount of Amberlite IR-120H resin in open glass vessel and subjected to the microwave irradiation at low power setting (25%, 250 w) for 3–6 min, then allowed to cool. The reaction mixture was dissolved in ethanol and resin was filtered off. Finally the filtrate was evaporated to dryness in evaporator. The crude product was further recrystallized from ethanol. The analytical data are given in experimental section.

*2.9.2.1. 5-Methyl-((2r,6c-diphenylpiperidin-4-ylidene)hydrazono) thiazolidin-4-one (**15**).* Pale yellow powder, yield 96%, m.p: 216–217 °C; FT-IR (cm^{-1}) 1729 (C=O), 1608 (C2' = N), 1640 (C4=N), 1386 (N–H); ^{1}H NMR (δ, ppm, DMSO-d_6): 3.90 (d, 1H, H-2a), 3.78 (d, 1H, H-6a), 2.49 (t, 1H, H-3a), 2.37 (d, 1H, H-3e), 2.05 (t, 1H, H-5a), 3.52 (d, 1H, H-5e), 3.30 (bs, 1H, NH), 4.12 (m, 1H, H-5′), 1.46 (t, 3H, CH_3 at C-5′), 7.50 (d, 4H, *o*-H, *o*′-H), 7.35 (dd, 4H, *m*-H, *m*'-H), 7.26 (m, 2H, *p*-H, *p*'-H); ^{13}C NMR (δ, ppm, DMSO-d_6): 68.7 (C-2), 60.5 (C-6), 44 (C-3), 37.4 (C-5), 176.8 (C=O), 167.6 (C=N), 161.5 (C-2′), 144.0 (C-2″), 143.0 (C-6″) 128.2 (*o*-C, *o*-C′), 127.5 (*m*-C, *m*-C′), 126.5 (*p*-C, *p*-C′) and 18.9 (CH_3–C-5′) ppm. Anal. Found (cal.) for $C_{21}H_{22}N_4OS$ (%): C, 66.64 (66.60); H, 5.86 (5.84); N, 14.80 (14.87).

*2.9.2.2. 5-Methyl-((3t-methyl-2r,6c-diphenylpiperidin-4-ylidene) hydrazono)thiazolidin-4-one (**16**).* White powder, yield 98%, m.p: 230–231 °C; FT-IR (cm^{-1}) 1735 (C=O), 1637 (C2' = N), 1600 (C4=N), 1427 (N–H); ^{1}H NMR (δ, ppm, DMSO-d_6): 3.58 (d, 1H, H-2a), 3.91 (d, 1H, H-6a), 2.61 (m, 1H, H-3a), 2.23 (q, 1H, H-5a), 3.71 (dd, 1H, H-5e), 3.95 (q, 1H, H-5′), 1.62 (t, 3H, CH_3 at C-5′), 0.91 (t. 3H, CH_3 at C-3), 7.43 (d, 4H, *o*-H, *o*-H′), 7.30 (dd, 4H, *m*-H, *m*-H′), 7.20 (m, 2H, *p*-H, *p*-H′); ^{13}C NMR (δ, ppm, DMSO-d_6): 69.3 (C-2), 61.1 (C-6), 45.5 (C-3), 37.8 (C-5), 176.4 (C=O), 169.6 (C=N), 160.7 (C-2′), 143.6 (C-2″), 142.6 (C-6″), 128.4 (*o*-C, *o*'-C), 127.9 (*m*-C, *m*'-C), 126.7 (*p*-C, *p*'- C′), 42.2 (C-5′), 19.1 (CH_3–C-5′) and 11.9 (CH_3–C-3) ppm. Anal. Found (cal.) for $C_{22}H_{24}N_4OS$ (%): C, 67.34 (67.38); H, 6.16 (6.10); N, 14.27 (14.21).

*2.9.2.3. 5-Methyl-((3t-methyl-2r,6c-bis(p-chlorophenyl)piperidin-4-ylidene)hydrazono)thiazolidin-4-one (**17**).* White powder, yield 93%, m.p: 245–246 °C; FT-IR (cm^{-1}) 1731 (C=O), 1624 (C2' = N), 1630 (C4=N), 1389 (N–H); ^{1}H NMR (δ, ppm, DMSO-d_6): 3.54 (d, 1H, H-2a), 3.84 (d, 1H, H-6a), 2.58 (t, 1H, H-3a), 2.10 (t, 1H, H-5a), 3.51 (d, 1H, H-5e), 3.94 (m, 1H, H-5′), 1.65 (s, 3H, CH_3 at C-5′), 7.51 (d, 4H, *o*-H, *o*'-H), 7.41 (dd, 4H, *m*-H, *m*'-H); ^{13}C NMR (δ, ppm, DMSO-d_6): 60.5 (C-2), 59.0 (C-6), 44.7 (C-3), 33.2 (C-5), 12.2 (CH_3(eq)-C-3), 19.5 (CH_3–C-5′) 174.5 (C=O), 167.8 (C=N), 161.3 (C-2′), 141.8 (C-2″), 141.2 C-6″), 129.6 (*o*-C, *o*'-C′), 128.0 (*m*-C, *m*'-C), 131.7, 131.5 (*p*-C, *p*'-C), 42.3 (C-5′) ppm. Anal. Found (cal.) for $C_{22}H_{22}Cl_2N_4OS$ (%): C, 57.27 (57.24); H, 4.81 (4.79); N, 12.14 (12.18).

*2.9.2.4. 5-Methyl-((3t-methyl-2r,6c-bis(p-flurophenyl)piperidin-4-ylidene)hydrazono)thiazolidin-4-one (**18**).* White powder, yield 90%, m.p: 254–255 °C; FT-IR (cm^{-1}) 1731 (C=O), 1610 (C2' = N), 1648 (C4=N), 1373 (N–H); ^{1}H NMR (δ, ppm, DMSO-d_6): 3.55 (d, 1H, H-2a), 3.88 (d, 1H, H-6a), 2.57 (t, 1H, H-3a), 2.12 (t, 1H, H-5a), 3.15 (d, 1H, H-5e), 3.90 (m, 1H, H-5′), 1.62 (s, 3H, CH_3 at C-5′), 7.52 (d, 4H, *o*-H, *o*'-H), 7.16 (dd, 4H, *m*-H, *m*'-H); ^{13}C NMR (δ, ppm, DMSO-d_6): 60.7 (C-2), 58.9 (C-6), 44.7 (C-3), 33.2 (C-5), 174.2 (C=O), 167.3 (C=N), 160.7 (C-2′) 139.0 (C-2″, C-6″), 129.5 (*o*-C, *o*'-C), 114.5 (*m*-C, *m*'-C), 162.0, 160.0 (*p*-C, *p*'-C), ppm. Anal. Found (cal.) for $C_{22}H_{22}F_2N_4OS$ (%): C, 61.67 (61.61); H, 5.17 (5.23); N, 13.08 (13.02).

*2.9.2.5. 5-Methyl-((3t-methyl-2r,6c-bis(p-methylphenyl)piperidin-4-ylidene)hydrazono)thiazolidin-4-one (**19**).* White powder, yield 89%, m.p: 244–245 °C; FT-IR (cm^{-1}) 1740 (C=O), 1645 (C2' = N), 1628 (C4=N), 1383 (N–H); ^{1}H NMR (δ, ppm, DMSO-d_6): 3.63 (d, 1H, H-2a), 3.85 (d, 1H, H-6a), 2.58 (t, 1H, H-3a), 2.17 (t, 1H, H-5a), 3.35 (d, 1H, H-5e), 3.93 (m, 1H, H-5′), 1.63 (s, 3H, CH_3 at C-5′), 0.91 (s, 3H, CH_3–C-3), 7.40 (d, 4H, *o*-H, *o*'-H′), 7.14 (dd, 4H, *m*-H, *m*'-H′); ^{13}C NMR (δ, ppm, DMSO-d_6): 69.4 (C-2), 59.8 (C-6), 43.0 (C-3), 33.9 (C-5), 174.5 (C=O), 168.1 (C=N), 161.4 (C-2′) 136.1 (C-2″, C-6″), 126.6 (*o*-C, *o*'-C′), 127.9 (*m*-C, *m*'-C), 128.7 (*p*-C, *p*'-C), 161.4 (C-2′) 22.7 (*p*-CH_3) ppm. Anal. Found (cal.) for $C_{24}H_{28}N_4OS$ (%): C, 68.54 (68.61); H, 6.71 (6.65); N, 13.32 (13.37).

*2.9.2.6. 5-Methyl-((3t-methyl-2r,6c-bis(p-methoxyphenyl)piperidin-4-ylidene)hydrazono) thiazolidin-4-one (**20**).* White powder, yield 87%, m.p: 240–241 °C; FT-IR (cm^{-1}) 1739 (C=O), 1646 (C2' = N), 1632 (C4=N), 1389 (N–H); ^{1}H NMR (δ, ppm, DMSO-d_6): 3.56 (d, 1H, H-2a), 3.83 (d, 1H, H-6a), 2.55 (t, 1H, H-3a), 2.18 (t, 1H, H-5a), 3.45 (d, 1H, H-5e), 3.90 (m, 1H, H-5′), 1.60 (s, 3H, CH_3 at C-5′), 0.98 (s, 3H, CH_3–C-3), 7.36 (d, 4H, *o*-H, *o*'-H), 6.90 (dd, 4H, *m*-H, *m*'-H); ^{13}C NMR (δ, ppm, DMSO-d_6): 69.0 (C-2), 59.5 (C-6), 43.1 (C-3), 33.9 (C-5), 173.6 (C=O), 167.8 (C=N), 161.2 (C-2′) 132.4 (C-2'', C-6''), 129.8 (*o*-C, *o*'-C), 113.6 (*m*-C, *m*'-C), 158.4 (*p*-C, *p*'-C), 161.2 (C-2′), 54.9 (*p*-OCH_3) ppm. Anal. Found (cal.) for $C_{24}H_{28}N_4O_3S$ (%): C, 63.94 (63.90); H, 6.21 (6.25); N, 12.38 (12.34).

*2.9.2.7. 5-Methyl-((3,5-dimethyl-2r,6c-diphenylpiperidin-4-ylidene) hydrazono)thiazolidin-4-one (**21**).* White powder, yield 82%, m.p: 238–239 °C; FT-IR (cm^{-1}) 1735 (C=O), 1637 (C2' = N), 1600 (C4=N), 1427 (N–H); ^{1}H NMR (δ, ppm, DMSO-d_6): 4.10 (d, 1H, H-2a), 3.78 (d, 1H, H-6a), 2.71 (t, 1H, H-3a), 2.95 (d, 1H, H-5e), 3.90 (m, 1H, H-5′), 1.60 (s, 3H, CH_3 at C-5′), 7.44, 7.42 (d, 4H, *o*-H, *o*-H′), 7.31 (dd, 4H, *m*-H, *m*-H′), 7.26 (m, 2H, *p*-H, *p*-H′), 0.92 (3H, CH_3 – C-2); ^{13}C NMR (δ, ppm, DMSO-d_6): 69.6 (C-2), 60.1 (C-6), 43.5 (C-3), 33.8 (C-5), 173.6 (C=O), 169.5 (C=N), 160.7 (C-2′) 143.7, 143.5 (C-2″, C-6″), 129.1 (*o*-C, *o*'-C), 128.1 (*m*-C, *m*'-C), 127.4 (*p*-C, *p*'- C′), 11.8 (CH_3–C-3), 11.0 (CH_3 – C-5) ppm. Anal. Found (cal.) for $C_{23}H_{26}N_4OS$ (%): C, 67.95 (67.90); H, 6.45 (6.50); N, 13.78 (13.72).

2.10. Biological activities

2.10.1. Antibacterial study

The newly synthesized compounds were evaluated for their *in vitro* antibacterial activity against *E. coli* (ATCC-25922), *S. aureus* (ATCC-25923), *P. aeruginosa* (ATCC-27853), the clinical isolate of *K.pneumoniae* and *S. pyogenes* bacterial strains by serial plate dilution method. The compounds were dissolved in 100% dimethyl sulfoxide (DMSO) and was diluted further (a twofold serial dilution) using Muller Hinton broth. Serial dilutions of the drug in Muller-Hinton broth was taken in tubes and their pH were adjusted to 7.2–7.4 using phosphate buffer. A standardized suspension of the test bacterium (as per the Clinical and Laboratory Standards Institutes (CLSI) guidelines) was inoculated and incubated for 18–24 h at 37 °C [21]. The minimum inhibitory concentration (MIC) was noted by seeing the lowest concentration of the drug at which there was no visible growth. The activity of each compound was compared with Streptomycin as standard [22]. MIC (μg/mL) was determined for **15**–**21** and the corresponding results are summarized in Table 6**.**

2.10.2. Anti-tuberculosis study

All the newly synthesized compounds were screened for their *in vitro* antimycobacterial activity against *M. Tuberculosis* $H_{37}Rv$ ATCC 27294, by Resazurin Assay method [23] and their MIC values were determined. The standard drug isoniazid (INH) was used as a reference. The screening results of the title compounds **15**–**21** reported in Table 6. M. Tuberculosis strains were grown in

Table 1
Synthesis of compounds **15**–**21** in Microwave irradiation and conventional methods.

S. No	Compounds	Micro Wave Irradiation			Conventional Method		
		Solvent	Reaction Time (Mins.)	Yield (%)	Solvent	Reaction Time (Hrs)	Yield (%)
1	16	Dry[a]	>10	NP	Methanol[a]	>6	NP
2	16	Methanol[b]	>10	50	Methanol[b]	>4	Trace
3	16	Ethanol[b]	>10	50	Ethanol[b]	4	80
4	16	Amberlit IR-120H	5	97	Ethanol[c]	4	90
5	15	Amberlit IR-120H	6	96	Ethanol[c]	5	89
4	17	Amberlit IR-120H	5	93	Ethanol[c]	5	85
5	18	Amberlit IR-120H	5	90	Ethanol[c]	5	85
6	19	Amberlit IR-120H	6	89	Ethanol[c]	5	78
7	20	Amberlit IR-120H	5	87	Ethanol[c]	5	76
8	21	Amberlit IR-120H	5	75	Ethanol[c]	5	69

[a] without catalyst.
[b] Sodium Acetate anhydrous.
[c] Amberlit IR-120H.

Table 2
Correlations in the COSY and NOESY spectra **16**.

Protons	Correlations in the COSY spectrum	Correlations in the NOESY Spectrum
7.43 (*o*-H, *o*'-H)	7.30 (*m*-H, *m*'-H)	3.58 (H-2a), 3.91 (H-6a) 2.23 (H-5a)
7.30 (*m*-H, *m*'-H)	7.43 (*o*-H, *o*'-H), 7.20 (*p*-H, *p*'-H)	7.43 (*o*-H, *o*'-H), 7.20 (*p*-H, *p*'-H)
7.20 (*p*-H, *p*'-H)	7.30 (*m*-H, *m*'-H)	7.30(*m*-H, *m*'-H)
3.95 (H-5′)	1.62 (CH_3 at C-5′)	1.62 (CH_3 at C-5′)
3.58 (H-2a)	0.91 (CH_3e)	7.43 (*o*-H), 0.91 (CH_3e)
2.23 (H-5a)	3.91 (H-6a), 3.71 (H-5e)	7.43 (*o*'-H), 3.71 (H-5e)
3.71 (H-5e)	2.23 (H-5a)	2.23 (H-5a)
3.91 (H-6a)	2.23 (H-5a), 3.71 (H-5e)	7.43 (*o*'-H), 3.71 (H-5e)
0.91 (CH_3e)	3.58 (H-2a)	7.43 (*o*-H), 3.58 (H-2a)
1.62 (CH_3 at C-5′)	3.95 (H-5′)	7.43 (*o*-H), 2.23 (H-5a)

Table 3
Correlations in the HSQC and HMBC spectra 16.

^{13}C Chemical shift (δ ppm)	Correlation in the HSQC spectrum	Correlation in the HMBC spectrum
176.4	–	1.62 (CH_3–C5') 3.95 (H-5′)
169.6	–	0.91 (CH_3–C3), 3.71 (H-5e),, 2.23 (H-5a), 3.58 (H-2a)
143.6	–	7.30 (*m*, *m*′ –H), 3.58 (H-2a)
142.6		7.36 (*m*, *m*′ –H), 3.91 (H-6a)
128.4	7.43 (*o*-H, *o*'-H)	7.20 (*p*, *p*′ –H)
127.9	7.30 (*m*, *m*′ –H)	7.43 (*o*-H, *o*'-H)
126.7	7.20 (*p*, *p*′ –H)	7.43 (*o*-H, *o*'-H)
69.3	3.58 (H-2a)	7.43 (*o*-H), 2.61 (CH_{3a})
61.1	3.91 (H-6a)	7.43 (*o*'-H), 2.23 (H-5a),
45.5	2.61 (H-3a)	0.91 CH_3(e)
42.2	3.59 (H-5′)	1.62 (CH_3 at C-5′)
37.8	2.23 (H-5a)	3.71 (H-5e), 3.58 (H-2a)
11.9	0.91 CH_3(e)	3.58 (H-2a)
19.1	1.62 (CH_3 at C-5′)	3.95 (H-5′)

Table 4
Crystal data and structure refinement of compound **21**.

Empirical Formula	C_{23} H_{26} N_4OS
Formula weight	406.54
Temperature	293 K
Wavelength	0.71073 Å
Crystal system, space group	Triclinic, Pī
Unit cell dimension	a = 10.1048 (5) Å α = 92.131 (3)° b = 11.2862 (5) Å β = 106.382 (2)° c = 12.3156 (5) Å γ = 109.757 (3)°
Volume	1254.45 (10) $Å^3$
Z, density	2, 1.076 Mg/m^3
Absorption coefficient	0.147 mm^{-1}
Crystal size	0.22 × 0.18 × 0.16 mm
Reflections collected	23239/6309 [R (int) = 0.0232]
Absorption correction	Multi-Scan SADABS
Refinement method on	Full-materix least square on F^2
w$R(F^2)$	0.2648
CCDC No	1530656

Middlebrook 7H9 broth, Supplemented with 10% OADC. The culture was diluted to McFarland 2 standard with the same medium. From this, 50 mL of this culture was added to 150 mL of fresh medium in 96 well microliter plates. Stock solutions (2 μg/mL) of the test compounds were prepared in dimethylformamide (DMF). The compounds were tested at 10 and 100 μg/mL concentrations. Further, the second level testing was carried out at concentrations 0.3125, 0.625, 1.25, 2.5 and 5 μg/mL. Control tubes had the same volumes of DMF without any substrate. Isoniazid (INH) was used as there reference drugs. After incubation at 37 °C for 7 days, 20 mL of 0.01% Resazurin in water was added to each tube. Resazurin, a redox dye, is blue in the oxidized state and turns pink when reduced by the growth of viable cells. The control tubes showed a colour change from blue to pink after 1 h at 37 °C. Compounds which prevented the change of colour of the dye was considered to be inhibitory to M. Tuberculosis. Inoculums size of 0.01 mL was taken and sub cultured on Middlebrook 7H10 plates. After incubation of 7 days, number of colonies were counted in control and test plates for calculation of strength (in %) of the compound in

Table 5
Selected Bond lengths, Bond angles and Torsional angles for **21**.

Bond lengths [A]	Torsional angles [°]	
S1–C20 1.752(3)	C16–N1–C15–C6 170.5(2)	C23–N4–C20–S1 -2.6(4)
S1–C21 1.815(4)	C16–N1–C15–C13 64.6(3)	C21–S1–C20–N3 -178.4(4)
N1–C15 1.452(3)	C15–N1–C16–C12 172.5(2)	C21–S1–C20–N4 -0.3(3)
N1–C16 1.469(4)	C15–N1–C16–C17–63.9(3)	N1–C16–C12–C7 50.4(4)
C19–N2 1.279(3)	N2-19-C17- C18 1.9(4)	C17–C16–C12–C7 -71.1(4)
C19–C13 1.507(4)	C13–C19–C17–C18–177.13)	N1–C16–C12–C11–130.7(3)
C19–C17 1.511(4)	N2–C19–C17–C16 127.7(3)	C17–C16–C12–C11 107.7(3)
C15–C6 1.513(4)	C13–C19–C17–C16–51.3(3)	C5–C6–C1–C2 -1.1(5)
C15–C13 1.541(4)	N1–C16–C17–C19 54.1(3)	C1–C6–C5–C4 0.8(6)
C16–C12 1.509(4)	C12–C16–C17–C19 175.9(2)	C15–C6–C5–C4 -179.0(4)
C16–C17 1.538(4)	N1–C16–C17–C18–179.4(2)	C7–C12–C11–C10–0.5(5)
C17–C18 1.520(4)	C12–C16–C17–C18–57.6(3)	C16–C12–C11–C10–179.3(3)
N2–N3 1.413(3)	C13–C19–N2–N3 -4.2(4)	C11–C12–C7–C8 0.8(5)
C6–C5 1.382(4)	C1–C19–N2–N3 176.9(2)	C16–C12–C7–C8 179.6(3)
C6–C1 1.383(4)	N1–C15–C6–C5 -14.6(4)	C6–C1–C2–C3 0.7(5)
C13–C14 1.528(5)	C13–C15–C6–C5 108.9(3)	C20–N4–C23–O1 -177.9(4)
N4–C23 1.346(5)	N1–C15–C6–C1 165.7(3)	C20–N4–C23–C21 4.7(5)
N4–C20 1.378(4)	C13–C15–C6–C1 -70.8(3)	O1–C23–C21–C22 46.3(8)
N3–C20 1.272(4)	N2–C19–C13–C14 107.2(3)	N4–C23–C21–C22–136.3(5)
C22–C21 1.416(8)	C17–C19–C13–C14–73.9(3)	O1–C23–C21–S1 178.2(4)
C12–C7 1.382(5)	N2–C19–C13–C15–127.6(3)	N4–C23–C21–S1 -4.4(5)
C12–C11 1.384(5)	C17–C19–C13–C15 51.3(3)	C20–S1–C21–C22 136.2(5)
C1–C2 1.392(5)	N1–C15–C13–C19–55.1(3)	C20–S1–C21–C23–2.5(4)
O1–C23 1.216(4)	C6–C15–C13–C19–179.9(2)	C6–C5–C4–C3 -0.1(7)
C5–C4 1.387(5)	N1–C15–C13–C14 69.0(3)	C5–C4–C3–C2 -0.3(7)
C11C10 1.380(5)	C6–C15–C13–C14–55.8(3)	C1–C2–C3–C4 0.0(6)
C7–C8 1.377(4)	C19–N2–N3–C20 160.8(3)	C12–C11– C10–C9 0.0(6)
C2–C3 1.367(5)	N2–N3–C20–N4 178.8(3)	C11–C10–C9–C8 0.2(7)
C23–C21 1.545(7)	N2–N3–C20–S1 -3.2(4)	C10–C9–C8–C7 0.1(6)
C4–C3 1.365(5)	C23–N4–C20–N3 175.7(3)	C12–C7–C8–C9 -0.6(5)

Table 6
In vitro antibacterial and antimycobacterial activities of compounds **15**–**21**.

Compounds	R	Minimum inhibitory concentration (MIC) in μg/mL					MTB[a] (% of inhibition)	
		S. aureus	S. pyogenes	P. aeruginosa	K. pneumoniae	E.coli	Preliminary (10 μg/mL)	Second level (2.5 μg/mL)
15	H	3.12	3.12	12.5	6.25	12.5	0	–
16	H	1.6	6.25	12.5	1.6	3.125	0	–
17	*p*-Cl	0.8	1.0	0.2	0.1	0.2	95	94
18	*p*-F	0.8	0.8	0.4	0.2	0.2	90	90
19	*p*-CH_3	3.25	1.6	6.25	6.25	3.125	0	–
20	*p*-OCH_3	1.6	3.125	3.125	3.125	3.125	0	–
21	H	12.5	6.25	12.5	6.25	12.5	0	–
Streptomycin		1.0	0.4	0.4	0.05	0.025	–	
INH	–	–	–	–	–		>95	>95

[a] Percentage of inhibition against M. Tuberculosis $H_{37}Rv$.

question which was effective in reducing significant population in initial inoculums.

3. Results and discussion

3.1. Chemistry

A new series of piperdione derivatives, incorporating an important pharmacophore (thiazolidin-4-one group), were synthesized by cyclization of thiosemicarbazones (**8**–**14**) with ethyl 2-bromopropionate. All the parent 3/5-alkyl-2*r*,6*c*-diarylpiperidin-4-ones were prepared by the condensation of ketones, aldehydes and ammonium acetate in 1:2:1 ratio respectively, following the procedure of Noller and Baliah [24]. The second step of the synthesis involved the preparation of a series of thiosemicarbazones **8**–**14** by acid catalyzed condensation of thiosemicarbazide with 3/5-alkyl-2*r*,6*c*-diarylpiperidin-4-ones **1**–**7** as shown in Scheme 1.

Herein, we report for the first time a solvent free reaction for a combinatorial synthesis of thiazolidin-4-one framework under microwave irradiation in presence of Amberlite IR-120H resin. Initially, we have added a catalytic amount of Amberlite IR-120H resin to equimolar mixture of 2,6-diarypiperidin-4-ones (**1**–**8**), thiosemicarbazide and ethyl-2-bromopropionate in a microwave vessel. Then the reaction mixture was placed in the microwave oven for 3–6 min at 250 W. The progress of the reaction was monitored by TLC. After complete conversion into the product, the resin was filtered off and the filtrate was evaporated to dryness in the evaporator. The crude product was further recrystallized from ethanol. In this new method, the reaction has been carried out efficiently in a shorter time.

In order to establish the optimized reaction conditions, the reaction of 3*t*-methyl-2*r*,6*c*-diphenylpiperidin-4-one (**2**) (1 mmol), thiosemicarbazide (1 mmol), and ethyl 2-bromopropionate (1 mmol) under different conditions such as nature of solvent, type and amount of catalyst reaction time and reaction temperature were examined (Table 1). Initially, the three components were heated in methanol (Entry 1) under conventional heating at reflux temperature yielding the final product is very low. Similar results were obtained under microwave irradiation, when no significant change in the yield was observed. The high reaction temperature and same yield discouraged us to further utilize the method. In continuations, we ardently employed ethanol as reaction medium with sodium acetate anhydrous catalyst both under micro wave as well as conventional heating method but low reaction yield and prolonged reaction time disappointed us. The reaction condition was further modified and improved by utilizing *p*-toluenesulphonic acid as a catalyst in ethanol as reaction medium leading to decrease in reaction time as well as increase in yield in both conditions. But still, the reaction conditions did not satisfy our objective due comparatively long reaction time and low yields. Thus our focus toward utilizes of environmentally benign catalyst to accomplish the one-pot protocol for the synthesis of desired molecules. Thus, Amberlit IR-120H promoted reaction (entry 4) was carried out under conventional and micro wave heating at 80 °C which rendered encouraging results with evident increase in yield as well as striking decrease in reaction time, additional rise in temperature up to 100 °C improved the results in terms of yield and reaction time. However, further increase in temperature above 100 °C accounted no improvements in the outcome. Thus this methodology was generalized to synthesize the other derivatives (Table 1). The catalytic efficiency of Amberlit IR-120H was also studied by utilizing the catalyst obtained from previous run up to 5 successive

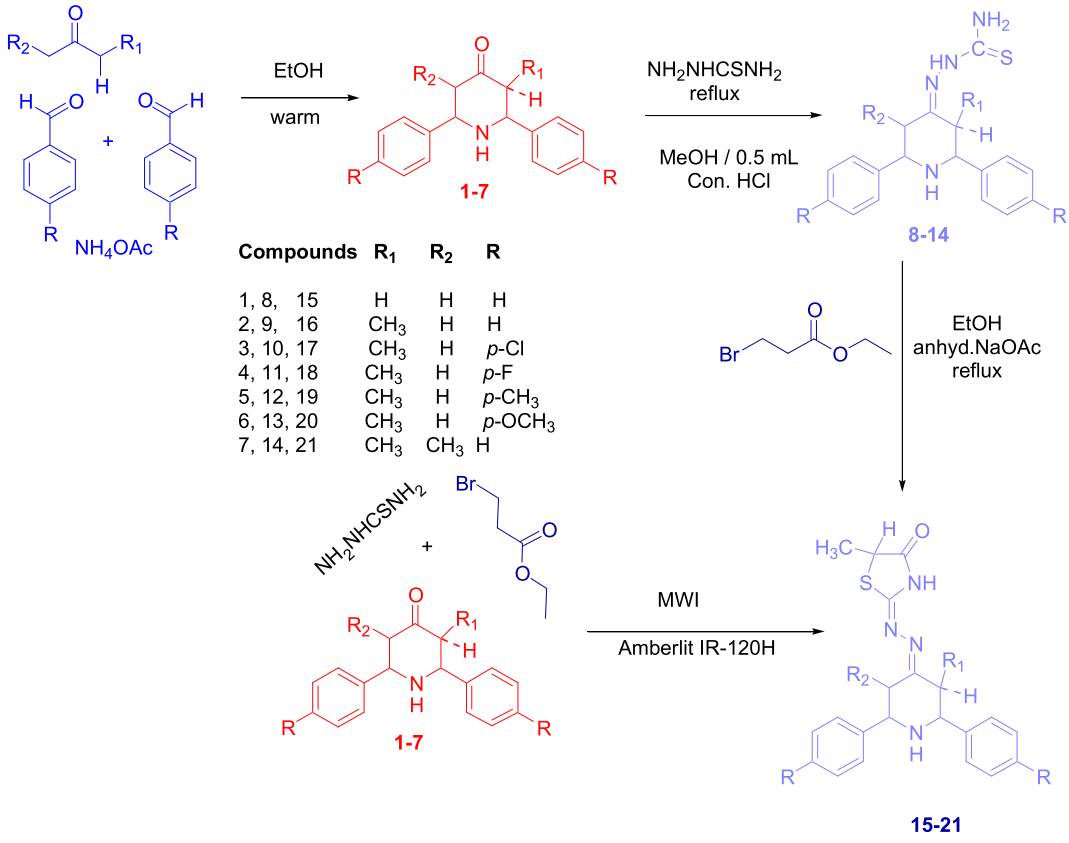

Scheme 1. Schematic diagram showing the synthesis of title compounds **15**–**21**.

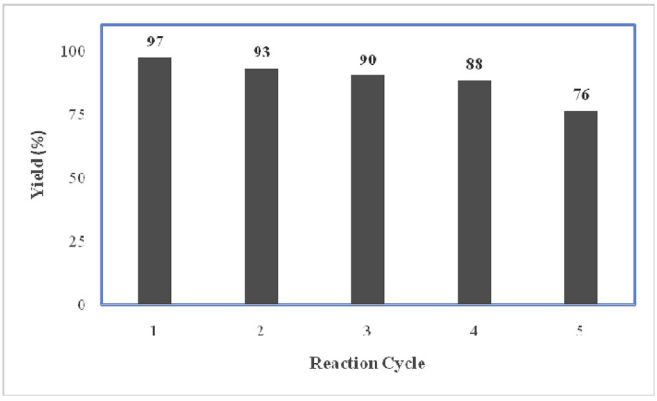

Fig. 1. Reusability of Amberlite IR-120H for the synthesis of **16**.

reaction cycles, which showed that there was notable decrease in the efficiency of the catalyst only after four successive cycles. As depicted in Fig. 1, the catalyst promoted better reusability and thus can be reused for at least four times.

Therefore, it has been concluded that Amberlite IR-120H mediated solvent free techniques are most efficient and selective in terms of reaction time, ease of isolation and yield of the product. The effective of microwave irradiation evaluate with the comparison of conventional reaction condition. This result clearly indicates that the effect of microwave is not merely thermal. It could be expected that the application of microwave irradiation causes easy excitation of electronic energy levels and thus leads to better yield and their analytical data are fit well with their proposed molecular formula.

3.2. Numbering and designation of atoms

The numbering of carbon and hydrogen atoms of the compound is shown in Fig. 2. The *ipso* carbons of the aryl groups at C-2 and C-6 are designated as C-2″ and C-6''. The other carbons of the aryl group at C-2 are denoted as *o*, *m*, *p* carbons and those of the aryl group at C-6 are denoted as *o'*, *m'*, *p'* carbons. The thiazolidine ring carbons are denoted as C-2′, C-4′ and C-5'. The protons are denoted accordingly. For example, the benzylic proton at C-2 is denoted as H-2 that the C-5′ is denoted as H-5′ and so on. The methylene protons at C-5 are denoted as H-5a and H-5e assuming chair conformation for the piperidine ring.

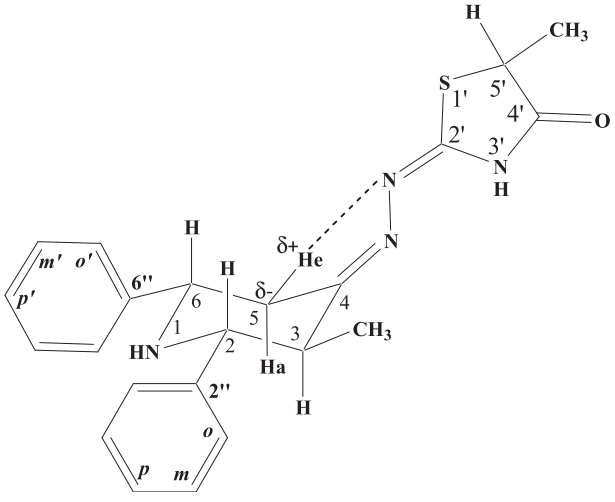

Fig. 2. Numbering of carbons, Non-bonded interaction and Conformation of the compound **16.**

3.3. IR spectral studies

In the FT-IR spectrum, the band around 3162 cm^{-1} indicated the presence of NH of the thiazolidine ring. The compounds (**15**–**21**) revealed bands at 1720–1735 cm^{-1} indicating the presence of a carbonyl group (-C═O). The compounds displayed absorption bands corresponding to the C═C aromatic ring at 1480–1580 cm^{-1}. The important characteristic FT-IR bands of the compounds are summarized in experimental section.

3.3.1. Proton and ^{13}C NMR spectral analysis of compound (16)

In order to analysis the spectral assignments of synthesized novel compounds **15**–**21**, we have chosen compound **16** as the representative compound. The proton chemical shift assignment has been made based on characteristic signal positions of functional groups, spin multiplicity, and comparison with those of parent ketones. The ^{1}H and ^{13}C signals for the remaining compounds were assigned by comparison with **16** using known effects [25] of the Cl, CH_3 and OCH_3 substituent's in the aryl rings.

In the ^{1}H NMR spectrum of **16**, there is a doublet at 7.43 ppm, corresponding to four protons, which is attributed to the *ortho* protons (*o*-H and *o*′-H). There is one quartet at 7.30 ppm, corresponding to four protons. This signal is an overlap of two triplets, and it should be due to the *meta* protons (*m*-H and *m*′-H). There is a quartet at 7.20 ppm, corresponding to two protons. This signal should be due to the *para* protons (*p*-H and *p*′-H) of the phenyl groups. The *ortho* protons appear at a higher frequency than other aromatic protons due to the de-shielding by the lone pair of nitrogen atom.

There are two doublets of doublets at 3.91 and 3.58 ppm, each corresponding to one proton. These signals are due to the bezylic protons of H-6a and H-2a. There is a quartet at 3.95 ppm, corresponding to one proton, which is attributed to the thiazolidine H-5′ proton.

There is a doublet of doublet at 3.71 ppm, corresponding to one proton. This should be due to H-5e. There is a multiplet at 2.61 ppm, corresponding to one proton. This must be due to the H-3a proton. There is a triplet at 2.23 ppm, corresponding to one proton. This should be due to the H-5a proton.

There are two triplets 1.62 and 0.91 ppm, each corresponding to three protons. The signal at 1.62 ppm is methyl proton at (CH_3–C-5′) of thiazolidine. The remaning one is methyl proton of piperidine at C-3. By careful examination the thiazolidine and piperidone NH protons are merged with solvent and H-2a signals.

To confirm the above assignment ^{1}H–^{1}H COSY and NOESY spectra have been recorded (Figs. 5 and 6 Supplementary Information). The observed correlations of **16** are given in Table 2. In the ^{1}H–^{1}H COSY (Fig. 3) (Fig. 5 in Supplementary Information) signal 3.95 ppm show correlation with 1.62 ppm. This correlation suggests that the signal at 3.95 ppm is due to H-5′ and that at 1.62 ppm is due to the CH_3 at C-5'. Also, there is correlation between the signals at 3.91 ppm and that at 2.25 and 3.58 ppm. These correlations suggest that the signals at 3.91, 3.58, 3.71 and 2.23 ppm are due to H-6a, H-2a, H-5e and H-5a respectively. It is seen that the *ortho* protons shows correlation with the signal at 7.30. The *ortho* protons can couple with only *meta* protons obviously, the signals at 7.43 ppm is due to *o*-H, *o*'-H and that at 7.30 ppm is due to *m*-H and *m*'-H. In the NOESY spectrum (Fig. 3) (Fig. 6 in Supplementary Information)) the signal for H-2a has NOE with the methyl protons at 0.91 ppm. Obviously, this signal should be due to the equatorial methyl protons because only the equatorial methyl protons can have NOE with

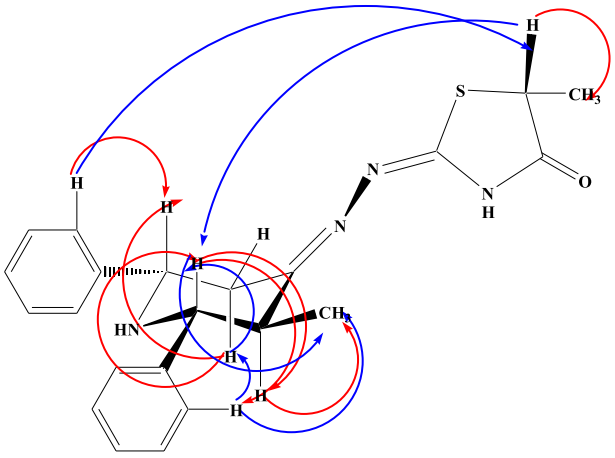

Fig. 3. COSY and NOESY NMR correlations of Compound **16**.

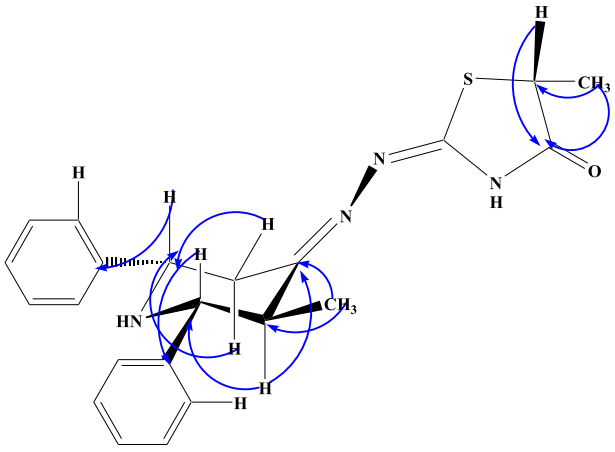

Fig. 4. HMBC NMR correlations of Compound **16**.

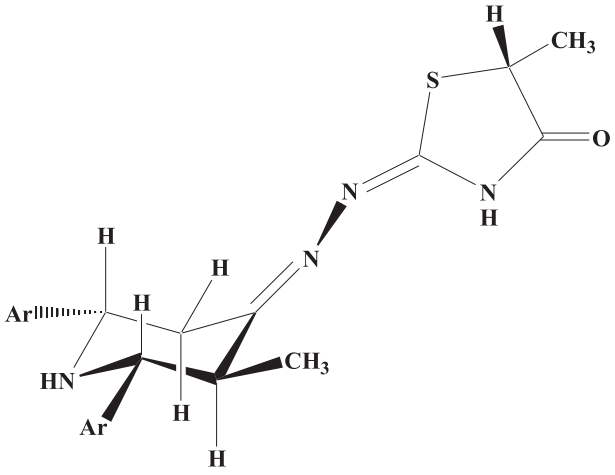

Fig. 5. Chair conformation of compound **16**–**21**.

the adjacent axial proton H-2a.

In **15** and **17**–**21**, assignments of the individual protons were made based on their multiplicities, position, integral values of the signals and by comparison with **16**. Due to the lone pair of electrons present in the piperidone nitrogen the *ortho* protons are

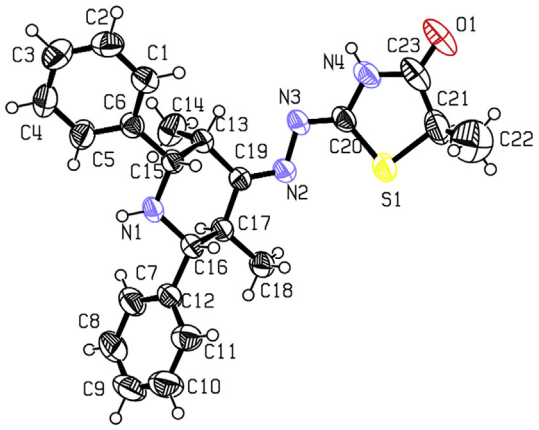

Fig. 6. ORTEP diagram of compound **21**.

deshielded, but the *meta* and *para* protons are shielded and resonated in the upfield region.

In order to assign the ^{13}C signals unambiguously HSQC and HMBC (Figs. 7 and 8 Supplementary Information) spectra have been recorded. The observed correlations in the HSQC and HMBC spectra are given in Table 3.

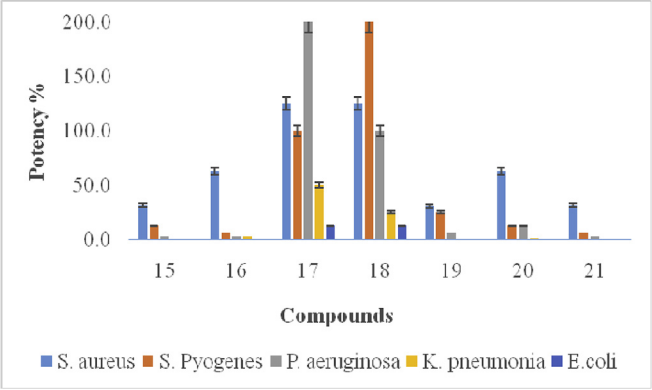

Fig. 7. Comparison of antibacterial potency of compounds **15**–**21** with *Streptomycin*.

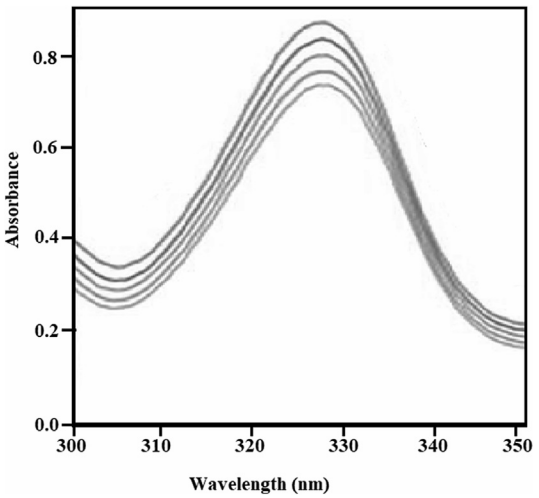

Fig. 8. UV absorption spectra of compound **17** in the presence of different concentrations of CT-DNA at pH 7.4 and room temperature.

There is a signal at 176.4 ppm. This signal has no correlation in the HSQC spectrum. In the HMBC spectrum, signal shows correlation with methyl proton at 1.62 ppm, H-5′ proton at 3.95 ppm. Hence, this signal must be due to the carbonyl carbon C-4'. There is a signal at 169.6 ppm. This signal is also has no correlation in the HSQC spectrum. In the HMBC spectrum (Fig. 4), this signal shows correlation with methyl protons at H-3, H-5a, H-5e, and H-2. Hence, this signal must be due to C-4. There are three other weak signals at 160.7, 143.6 and 142.6 ppm. These signals have no correlation in HSQC spectrum. These signals are due to the *ipso* carbons of the phenyl groups and thiazolidinone ring. The signals in the range 30–70 ppm could be assigned to the heterocyclic ring carbons. A set of signals in the upfield region 45.5 and 37.8 ppm are assigned to C-3 and C-5 carbons respectively. Among these two signals C-5 is shielded due to γ-*syn* effect. Similarly the C-2 and C-6 resonances were observed at 69.3 and 61.1 ppm respectively and the carbon C-6 is shielded due to extended γ-*syn* effect. The other signals are assigned based on the observed correlation in the HSQC and HMBC spectra. The ^{13}C signals for **15** and **17**–**21**, were assigned based on their multiplicities, position, intensity and comparison with **16**. The observed chemical shifts of **15**–**21** are given in experimental section.

3.3.2. Configuration about C(4) = N bond

In all compounds, the observed chemical shifts suggest that the chemical shift of H-5a is lower than that of H-5e by about 1.0 ppm. Also, C-3 as a much greater chemical shifts than C-5. Those observations suggest that the configuration about C_4=N bond is ***E***. In such a configuration the C-5 − H-5e bond will be polarized by γ-syn effect [26] so that H-5e gets a partial positive charge and C-5 gets a partial negative charge. The partial positive charge on H-5e deshields, if whereas the partial negative charge on C-5 shields it and H-5a (Fig. 2).

3.3.3. Analysis of coupling constants

The vicinal coupling constants are an important parameter for the conformational studies. The coupling constants for the protons of the piperidine ring could be determined précised for **16**.The observed coupling constants are as follows.

$J_{2a,3a}$ = 10.5 Hz; $J_{5a,6a}$ = 12.0 Hz; $J_{5a,6e}$ = 3.5 Hz; $J_{5a,5e}$ = 14.0 Hz.

Also in **17**–**20** the value of $J_{5a,6a}$ was about 12.0 Hz and that of $J_{5e,6a}$ was about 4.0 Hz in both the isomers. The observed vicinal coupling constants suggest that in **15**–**21** piperidine ring adopts chair conformation with equatorial orientations of the aryl groups and the methyl group at C-3 should be equatorial. (Fig. 5). The observations of large vicinal coupling constant values between 9.00 and 11.00 Hz ($J_{2a,3a}$) and 10.0–11.50 Hz ($J_{5a,6a}$). A small coupling constants of 2.5–3.5 Hz ($J_{6a,5e}$) for the protons of C-6 and C-2 of the compounds **16**–**21** indicate that the six-membered heterocyclic ring of compounds **15**–**21** adopts normal chair conformations (Fig. 5). Furthermore, equatorial position of phenyl group makes the chair conformation more rigid thereby preventing interconversion of one chair into another.

3.4. Single-crystal X-ray analysis of compound *21*

The structure of compound **21** in the solid state is established by single crystal x-ray analysis. It crystallizes into a triclinic lattice with space group P-1. Crystal data and structure refinement of compound **21** is shown in Table 4. The ORTEP diagram (Fig. 6) of 21 and displacement ellipsoids are drawn at 50% probability level. Selected bond length, angle and torsionals are given Table 5. The configuration about C=N bond C(19)–N(2) is **E** and the dihedral angle (N2–C19–C17–C16) is 127.7(3). The bond distance between C(19)–N(2) is 1.279(3)A° which shows its double bonded nature [27]. The ORTEP diagram reveals that the compound consists of two phenyl rings [C(15) and C(16)] and one thiazolidine ring [C(20)-N(4)-C(23)-C(21)-S(1)]. The dihedral angles of C16–N1–C15–C6 = 170.5(2), C15–N1–C16–C12 = 172.5(2), C12–C16–C17–C19 = 175.9(2), N1–C16–C17–C18 = −179.4(2), C6–C15–C13–C19 = −179.9(2), are indicate the two phenyl rings are in equatorially oriented. The observed dihedral angles of the piperidine ring C16–N1–C15–C13 = 64.6(3), C15–N1–C16–C17 = −63.9(3), C13–C19–C17–C16 = −51.3(3), N1–C16–C17–C19 = 54.1(3), C17–C19–C13–C15 51.3(3) and N1–C15–C13–C19 = −55.1(3) also support chair conformation of it.

3.5. Antibacterial activity

Antibacterial activity of title compounds were investigated against five different bacterial strains viz, *S. aureus*, *S. pyogenes*, *P. aeruginosa*, *K. pneumoniae* and *E. coli* using Streptomycin as reference, by serial dilution method. Results of antibacterial screening of compounds **15**–**21** indicate that the compounds showed MIC values between 0.1 and 12.5 μg/mL concentrations. It has been observed that the compounds **17** and **18** displayed substantial activity against *S. aureus, S. pyogenes* and *P. aeruginosa*. Amongst them, compound **18** showed better activity at 0.2 μg/mL against *S. pyogenes* which is more potent than the reference compound. The compound, **17** showed good activities at 0.1 μg/mL against *K. pneumonia* strain whereas all other compounds showed meager activity between 0.8 and 12.5 μg/mL. Only two compounds, **17** and **18** showed considerable activity against *E. coli* strain. Table 6 summarizes the antibacterial screening results (MIC μg/mL) of tested compounds along with that of standard. The antibacterial potency of the tested compounds compared with reference standard drug was calculated by the following equation.

$$= \frac{MIC\ \left(\frac{\mu g}{mL}\right)\ of\ reference\ drug}{MIC\ \left(\frac{\mu g}{mL}\right) of\ test\ compound} X100$$

It has been noticed that the structure of active compounds have chloro and fluoro groups. It is interesting to note that the activity decreased by two fold when 4-fluoro (**18**) was replaced by 4-methoxy group (**20**). The promising activity of the compounds is mainly attributed to the presence of fluoro and chloro substituted phenyl group present in piperidone system. The results suggest that the antibacterial activity is markedly influenced by substituent in phenyl ring (Fig. 7).

3.6. Anti-tubercular activity

Based on the encouraging results from the antibacterial screening, title compounds were further tested for their both preliminary and second level *in vitro* antimycobacterial activity against M. Tuberculosis $H_{37}Rv$, using isoniazid (INH) as standard drug. The results of preliminary level antimycobacterial screening of the tested compounds are tabulated in Table 6. From the results of preliminary antimycobacterial screening of compounds **15**–**21**, it has been observed that compounds **17** and **18** were active at concentration 10 μg/mL. Further, second level screening results revealed that compounds **17** and **18** were active at 2.5 μg/mL against M. Tuberculosis $H_{37}Rv$ strains. The remaining compound does not show the TB activity.

3.7. Interactions with calf thymus DNA

DNA is one of the targets for the studies of biologically important small molecules such as antimicrobial drugs. There is growing interest in investigating the interaction of small molecules with DNA for the rational design and construction of new and efficient drugs targeted to DNA. These studies are important and helpful for developing novel and more efficient drugs, which are attracting considerable attention in biomedical science. Thus, we decided to probe DNA-binding of the most effective molecule (**17**).

3.7.1. Absorption spectra of DNA in the presence of compound *17*

The UV–visible spectroscopy is one of the most suitable technique for determining the binding mode between the organic molecules and DNA helix [28,29]. As is well known, the binding interaction of DNA with a molecule often give rise to changes in the absorbance and in the position of peak [30]. Generally, hypochromism and red shift are associated with the intercalative binding mode between molecules and DNA, whereas hyperchromism is correlated with groove binding between host and guest.

The interaction of compounds **15**–**21** towards calf thymus DNA (CT-DNA) was investigated by UV–Vis spectroscopy in a solution of Tris-HCl buffer and DMSO (10%) and we have chosen compound **17** as the representative compound. (Fig. S2. Supplementary Information 15,16,18–21). The absorption spectrum of compound **17** with increasing concentration of (CT-DNA) was shown in Fig. 8**.** Upon increasing the concentration of CT-DNA to the **17**, decrease in absorption intensity was observed at 320 nm and no red shift was observed in the UV spectra, which represents that the binding mode is not the intercalative binding and these hyperchromism changes indicates that the binding mode of **17** to DNA might be groove binding [31]. Further experiments were performed to details study of the binding mode of CT-DNA with molecule **17.**

3.7.2. Steady state fluorescence

Fluorescence spectroscopy is a useful tool to study the interaction of drug molecules with CT-DNA. The intensity of fluorescence decreases due to a variety of molecular interactions, such as molecular rearrangements, energy transfer, excited-state reactions, and ground-state complex formation [32]. The decrease in intensity due to such molecular interactions is called fluorescence quenching. Fig. 9 shows the fluorescence emission spectra of **17** with CT-DNA at the emission maxima at 575 nm. Upon subsequent addition of CT-DNA, there is a gradual quenching of the fluorescence intensity without any significant change in the emission maxima which is direct evidence of the interaction between **17** and CT-DNA. To explain the results of fluorescence measurements quantitatively, the ratio of the peak fluorescence intensity in the presence and in the absence of CT-DNA (F/F0) has been plotted as a function of [DNA] using Stern-Volmer equation. Fig. 9A shows that with subsequent addition of DNA, the fluorescence intensity decreases which revels the interaction between compound 17 and CT-DNA is a minor groove-binding mode.

3.7.3. Competitive displacement assay

Ethidium bromide is a sensitive probe that intercalates within the base pairs of DNA. EB emits intense fluorescence in presence of DNA due to its strong intercalation between adjacent base pairs. As early reports that enhanced fluorescence of EB-DNA can be quenched by addition of second molecule [32,33]. So in order to confirm the mode of binding of 17 with the CT-DNA, we used EB as a probe. The fluorescence intensity of EB-DNA complex is shown in Fig. 10. The subsequent addition of **17** to EB-DNA system did not had any significant effect on the fluorescence intensity of EB-DNA complex proving that the mode of binding of **17** to CT-DNA is non-intercalative [34,35]. The quenching efficiency was determined by Stern - Volmer constant [36].

$$F_0 / F = 1 + KR \tag{2}$$

Where, F and F_0 are the fluorescence intensities in absence and presence of compound **17**. K is linear Stern-Volmer quenching constant. R is the ratio of the total concentration of **17** and CT-DNA. The K value was $2.85 \times 10^{-4}\,M^{-1}$, which indicates that the compound **17** interact with CT-DNA through groove binding.

3.7.4. Thermodynamic parameters

Thermodynamic parameters such as enthalpy change (ΔH), entropy change (ΔS) and free energy change (ΔG) are very important in defining these binding forces. The thermodynamic parameters were calculated with the help of the following equations.

$$LogK = \Delta H/(2.303RT) + \Delta S/(2.303R) \tag{3}$$

Here K and R are the binding constant and the universal gas constant ($8.314\,kJ\,K^{-1}mol^{-1}$) respectively. The values of ΔH and ΔS

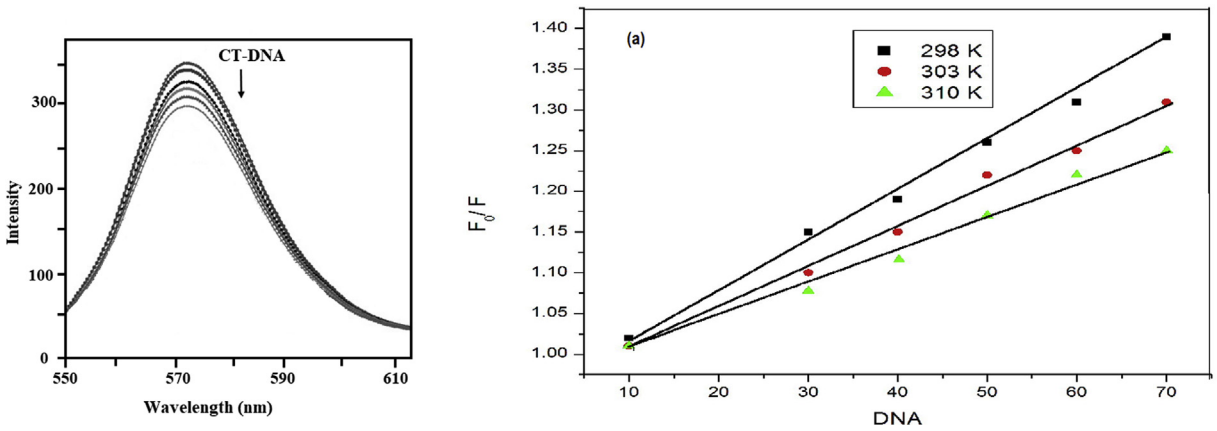

Fig. 9. (A) Fluorescence emission spectra of **17** (50 μM) in the presence of increasing concentrations of Ct-DNA (0–
80
μM). (B) Stern-Volmer plot for interaction of **17** with CT-DNA at 298 °C.

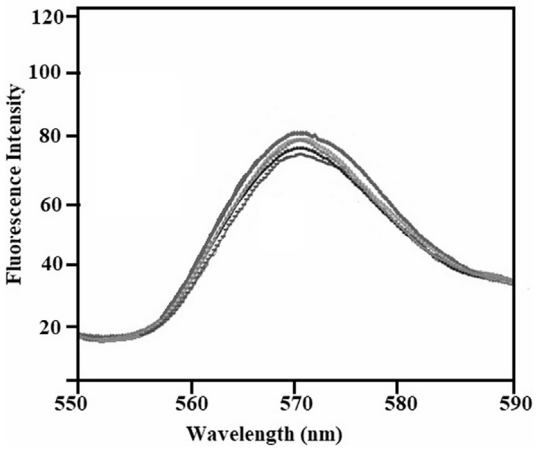

Fig. 10. Fluorescence spectra of the compound **17**-EB-DNA.

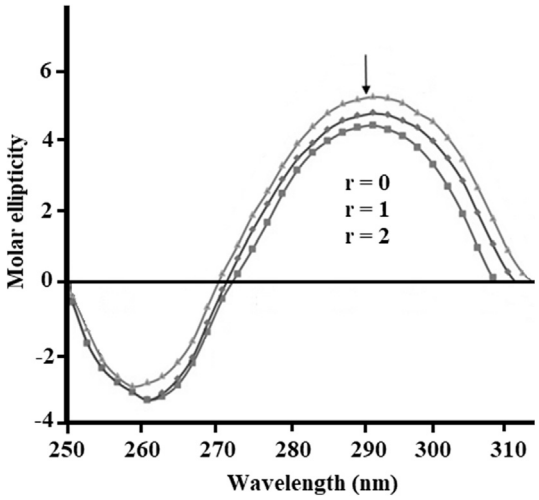

Fig. 11. The CD spectra of CT-DNA (50 μM) in the presence of **17** in 10 mM Tris HCl buffer (pH 7.4).

were obtained from the slope and intercept of the linear van't Hoff based on log Ka versus 1/T.

The value of free energy change (ΔG) was calculated from the following equation (Eq. (4))

$$\Delta G = \Delta H - T\Delta S \quad (4)$$

The negative value of ΔG means that the binding process is favorable and spontaneous. By calculating the values of ΔH and ΔS, the type of interaction between molecules and DNA can be identified [37]. According to the value of enthalpy change (ΔH) and entropy change (ΔS), the binding model of the compounds with DNA can be concluded: (1) ΔH < 0 and ΔS > 0, the main binding force is hydrogen bonds and hydrophobic interactions; (2) ΔH < 0 and ΔS < 0, the main binding force is hydrogen bonds and van der Waals forces; and (3) ΔH > 0 and ΔS > 0, hydrophobic interactions are major acting force [38,39]. In our study the calculated values for ΔH and ΔS are −8.11 and −3.58 kJmol^{-1} respectively at 293 K. The negative value of ΔG and ΔS suggesting that both hydrogen bonds and van der Waals forces played a major role in the binding of compounds to CT-DNA and contributed to the stability of the complex, and the binding process was spontaneous based on the negative free energy change.

3.7.5. Circular dichroism study

Circular dichroism spectroscopy is a powerful technique for observing the conformational changes in the CT-DNA during small molecules with DNA interactions The conformation and morphology of CT-DNA upon the interaction with small molecules including drugs is regularly investigated with the help of CD spectroscopy [40]. The CD spectrum of CT-DNA solution exhibits a typical B-form conformation with a positive peak at 290 nm for base stacking interaction and a negative peak at 266 nm for right-handed helicity [41]. Usually, groove binding and electrostatic interaction cause no or minimal perturbation on the base stacking as well as helicity bands of CT-DNA; whereas intercalation leads to the significant alteration in the intensity of these two bands and modulates the right-handed B-conformation of DNA [41]. The intensity as well as peak position of these two characteristic CD bands of CT-DNA negligibly altered upon the interaction with CT-DNA (Fig. 11 and Fig. S3**.** Supplementary Information **15,16,18**−**21**), which clearly suggests that compound may possibly interact with CT-DNA through groove binding mode. The result as observed from this study is an indication of groove binding of **17** to CT-DNA.

3.7.6. Cyclic voltammetry (CV) study

Cyclic voltammetry (CV) study was also carried out to investigate the nature of the binding interaction mode of the compound and CT-DNA. The experiment was carried out via titration of **17** with the CT-DNA solution and shown in Fig. 12. We have recorded CV of **17** (3×10^{-4} mol L^{-1}) in Tris-HCl buffer of pH 7.4. The drop of the voltammetric current with the addition of CT-DNA, might be due to slow diffusion of the equilibrium mixture of the free and CT-DNA bound compound in solution. From the figure, the anodic peak shifted positively while the cathodic peak shifted negatively, in the presence of CT-DNA and it indicates groove binding of compound **17** with the CT-DNA. Thus, we can conclude that cyclic voltameter experiments provide evidence of groove binding [42] and well correlated the results obtained from UV−Vis, fluorescence and Circular dichroism spectroscopic techniques. The groove binding mode of compound **17** to DNA was further confirmed by the results from DNA-Helix melting assay and viscosity assay.

3.7.7. DNA melting studies

The binding interaction of compound **17** with CT-DNA has further been confirmed from the DNA helix melting experiment.

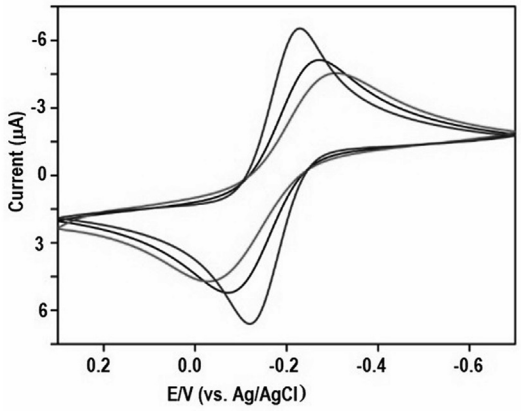

Fig. 12. Cyclic voltammogram of 50 μM of test compound in 10 mM tris-buffer, pH 7.4
at 50
mVs^{-1} scan rate without DNA and with DNA.

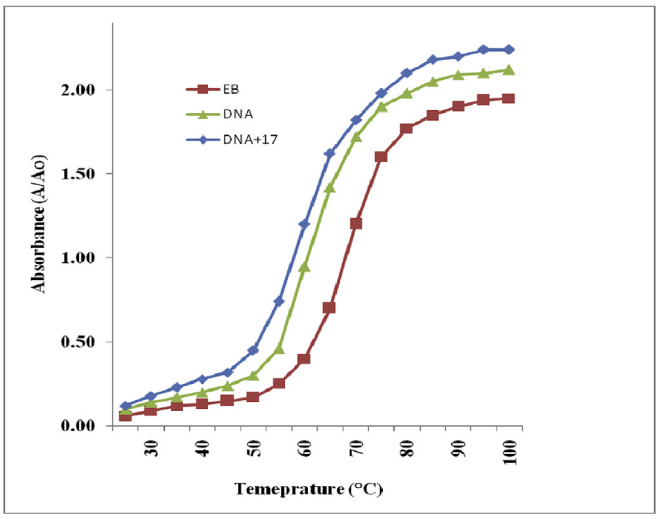

Fig. 13. Thermal melting profile of CT-DNA (50 μM) in the absence and presence of **17** (50 μM).

Melting temperature (Tm) is the temperature at which half of the DNA strands are separated into single strand and is correlated with stabilizing of DNA helix. In the presence of intercalators, the helix is stabilized and results in the increase in melting temperature by 8–12 °C [43]. On the other hand, groove binders do not cause an appreciable change in temperature value [44]. We have carried out the experiment to monitor the changes in the temperature of CT-DNA in the absence and presence of compound **17** and EB. By monitoring the absorbance at 260 nm as the transition midpoint of melting curve, the estimated melting temperatures appear to be 60.6 °C, 68.3 °C and 71.7 °C for CT-DNA, **17** and EB respectively (Fig. 13 and Fig. S4. Supplementary Information **15,16,18 and 19**). The experiment reveals that upon binding with EB (an intercalator) the Tm of CT-DNA is increased by 7.7 °C which is consistent with the literature. But an inappreciable change in temperature of DNA upon binding to **17**, conventionality supports the groove binding between these two.

3.7.8. *Viscometric study*

The viscosity measurements are highly sensitive and can provide conclusive evidence regarding the mode of interaction of small molecules with DNA. In order to establish the role of electrostatic interaction in **17**-DNA complex formation we studied the role of ionic strength by increasing concentration of NaCl. Due to its extreme sensibility it can give a significant evident concerning the binding mode of **17** and CT-DNA. Molecules that intercalate into the DNA require base pairs to separate in order to be accommodating into the helix resulting in the lengthening, unwinding and stiffening of the helix, thus increasing the viscosity of the DNA. On the other hand molecules that bind into grooves do not pose such steric requirements. If we titrate NaCl to drug-DNA solution, the electrostatic interaction between the drug and DNA is weakened and drug is released from the drug-DNA complex leading to an increase in the fluorescence intensity [45]. A viscosity plot of $(\eta/\eta 0)1/3$ versus [**17**]/[DNA] was obtained to detect any change in the viscosity of CT-DNA solution in the presence of **17**. The viscosities of CT-DNA with a series concentration of **17** were measured and shown in Fig. 14 (Fig. S5. Supplementary Information 15,16,18–21). In our study there is no such change observe which ruled out the chance of intercalation [46]. From Fig. 14 it is observe that with increasing the concentration of **17** there is no appreciable change in viscosity. This provides evidence that **17** interacts with CT-DNA through groove binding mode rather than intercalation.

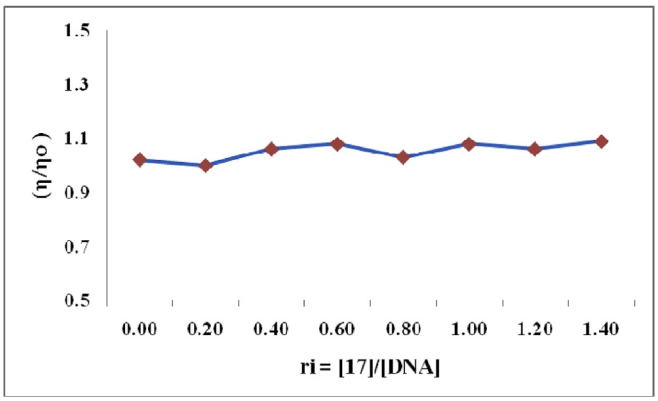

Fig. 14. Effect of increasing concentration of **17** on the relative viscosity of CT-DNA solution (50 μM).

4. Conclusion

We have successfully synthesized thiazolidin-4-one substituted piperidinone derivatives using Amberlit IR-120H resins under microwave irradiation in excellent yield. The structures of the compounds were elucidated by using FT-IR, NMR spectroscopy and single crystal x-ray method. The observed vicinal coupling constants suggest that in **15**–**21**, the piperidine ring adopts chair conformation with equatorial orientations of the aryl groups. All the synthesized compounds were screened for their *in vitro* antibacterial and anti-tubercular activities. Most of the compounds showed good antibacterial activity. Two leading compounds **17** and **18** displayed good antitubercular activity against mycobacterium tuberculosis H37Rv. The results indicated that compounds bearing the electron withdrawing group in the aryl moiety showed the highest antitubercular and antibacterial actives. UV–visible and fluorescence spectroscopy suggested the formation of minor groove between compounds with CT-DNA. From DNA melting study, CD spectral analysis and viscosity measurements the mode of binding was confirmed as non intercalative. Involvement of electrostatic interaction was ruled out by studying the effect of ionic strength. Our study could provide more help in understanding the binding mechanism of piperidone and related compounds with CT-DNA and the pharmacological effects of piperidone as well as designing the structure of new and efficient drug molecules.

Acknowledgements

The authors are thankful to SIF, Indian Institute of Science, Bangalore and to SAIF IIT- Madras for recording NMR spectra and elemental analysis of the compounds.

Appendix A. Supplementary data

Supplementary data to this article can be found online at https://doi.org/10.1016/j.molstruc.2019.126899.

References

[1] Global Tuberculosis Report 2016, World Health Organization, Geneva, Switzerland, 2016.
[2] Global Tuberculosis Report 2017, World Health Organization, Geneva, Switzerland, 2017.
[3] Global Tuberculosis Report 2013, World Health Organization, Geneva, Switzerland, 2013.
[4] Multidrug and Extensively Drug-Resistant TB (M, XDR-TB), Global Report on

Surveillance and Response, World Health Organization, Geneva, Switzerland, 2010, 2010.
[5] J. Ziemska, A. Rajnisz, J. Solecka, New perspectives on antibacterial drug research, Cent. Eur. J. Biol. 8 (2013) 943–957.
[6] S. Umamatheswari, B. Balaji, M. Ramanathan, S. Kabilan, Synthesis, antimicrobial evaluation and QSAR studies of novel piperidin-4-yl-5-spiro-thiadiazoline derivatives, Bioorg. Med. Chem. Lett 20 (2010) 6909–6914. https://doi.org/10.1016/j.bmcl.2010.10.002.
[7] M. Mangalam, C. Sebastian Antony Selvan, C. Sankar, Synthesis, stereochemical, structural, and biological studies of a series of N′-(2r,4c-diaryl-3-azabicyclo[3.3.1]nonan-9-ylidene)pyrazine-2-carbohydrazides, J. Mol. Struct. 1129 (2017) 305–312. https://doi.org/10.1016/j.molstruc.2016.09.033.
[8] K.C. Ruparelia, S. Lodhi, D.N. Ankrett, N.E. Wilsher, R.R.J. Arroo, G.A. Potter, K.J.M. Beresford, The synthesis of 4,6-diaryl-2-pyridones and their bioactivation in CYP1 expressing breast cancer cells, Bioorg. Med. Chem. Lett 29 (2019) 1403–1406. https://doi.org/10.1016/j.bmcl.2019.03.030.
[9] A.C. Tripathi, S.J. Gupta, G.N. Fatima, P.K. Sonar, A. Verma, S.K. Saraf, 4- Thiazolidinones: the advances continue, Eur. J. Med. Chem. 72 (2014) 52–77. https://doi.org/10.1016/j.ejmech.2013.11.017.
[10] M.M. Kamel, H.I. Ali, M.M. Anwar, N.A. Mohamed, A.M.M. Soliman, Synthesis, antitumor activity and molecular docking study of novel sulfonamide-Schiff's bases, thiazolidinones, benzothiazinones and their C-nucleoside derivatives, Eur. J. Med. Chem. 45 (2010) 572–580. https://doi.org/10.1016/j.ejmech.2009.10.044.
[11] A. Saeed, N.A. Al-Masoudi, M. Latif, Synthesis and Antiviral Activity of New Substituted Methyl [2-(arylmethylene-hydrazino)-4-oxo-thiazolidin-5-ylidene] acetates, Arch. Pharm. Chem. Life Sci. 346 (2013) 618–625. https://doi.org/10.1002/ardp.201300057.
[12] T. Srivastava, A.K. Gaikwad, W. Haq, S. Sinha, S.B. Katti, Synthesis and biological evaluation of 4-thiazolidinone derivatives as potential antimycobacterial agents, ARKIVOC ii (2005) 120–130. https://doi.org/10.3998/ark.5550190.0006.209.
[13] O.S. Afifi, O.G. Shaaban, H.A. Abd El Razik, S. El-Dine, A. Shams El-Dine, F.A. Ashour, A.A. El-Tombary, M.M. Abu-Seriec, Synthesis and biological evaluation of purine-pyrazole hybrids incorporating thiazole, thiazolidinone or rhodanine moiety as 15-LOX inhibitors endowed with anticancer and antioxidant potential, Bioorg. Chem. 87 (2019) 821–837. https://doi.org/10.1016/j.bioorg.2019.03.076.
[14] M.F. Ansari, D. Idrees, Md I. Hassan, K. Ahmad, F. Avecilla, A. Azam, Design, synthesis and biological evaluation of novel pyridine thiazolidinone derivatives as anticancer agents: targeting human carbonic anhydrase IX, Eur. J. Med. Chem. 144 (2018) 544–556. https://doi.org/10.1016/j.ejmech.2017.12.049.
[15] K. Hemlata, Sunil Kumar, P. Vishwakarma, M. Sharma, K.K. Saxena, Ashok Kumar, Synthesis and antipsychotic and anticonvulsant activity of some new substituted oxa/thiadiazolylazetidinonyl/thiazolidinonylcarbazoles, Eur. J. Med. Chem. 45 (2010) 2777–2783. https://doi.org/10.1016/j.ejmech.2010.02.060.
[16] S. Gujarathi, H.P. Hendrickson, G. Zheng, Amberlite IR-120H as an efficient and versatile solid phase catalyst for nucleophilic substitution of propargylic alcohols, Tetrahedron Lett. 54 (2013) 3550–3553. https://doi.org/10.1016/j.tetlet.2013.04.120.
[17] A. Paul, S. Bhattacharya, Chemistry and biology of DNA-binding small molecules, Curr. Sci. 102 (2012) 212–231. https://doi.jstor.org/stable/24083849.
[18] T.R. Gadek, J.B. Nicholas, Small molecule antagonists of proteins, Biochem. Pharmacol. 65 (2003) 1–8. https://doi.org/10.1016/S0006-2952(02)01479-X.
[19] G.M. Sheldrick, Acta Crystallogr. Phase annealing in SHELX-90: direct methods for larger structures 46 (1990) 467–473.
[20] G.M. Sheldrick, SHELXL-97, University of Gottingen, Goettingen, Germany, 1997.
[21] M07-A8, in: Methods for Dilution Antimicrobial Susceptibility Tests for Bacterial that Grow Aerobically, vol. 29, Approved Standard-eighth edition, 2009, pp. 1–10.
[22] R. Davis, A. Markham, J.A. Balfour, Ciprofloxacin, an updated review of its pharmacology, therapeutic efficacy and tolerability, Drugs 51 (1996) 1019–1074. https://doi.org/10.2165/00003495-199651060-00010.
[23] K.T. Neetu, S.T. Jaya, Resazurin reduction assays for screening of antitubercular compounds against dormant and actively growing Mycobacterium tuberculosis, Mycobacterium bovis *BCG and* Mycobacterium smegmatis, J. Antimicrob. Chemother. 60 (2007) 288–293. https://doi.org/10.1093/jac/dkm207.
[24] C.R. Noller, V. Baliah, The preparation of some piperidine derivatives by the mannich reaction, J. Am. Chem. Soc. 70 (1948) 3853–3855. https://doi.org/10.1021/ja01191-092.
[25] R.M. Silverstein, F.X. Webster, In Spectroscopic Identification of Organic Compounds, sixth ed., John Wiley, Singapore, 2002.
[26] C.N. Sudhamani, H.S. Bhojya Naik, T.R. Ravikumar Naik, M.C. Prabhakara, Synthesis, DNA binding and cleavage studies of Ni(II) complexes with fused aromatic N-containing ligands, Spectrochim. Acta, Part A 72 (2009) 643–647. https://doi.org/10.1016/j.saa.2008.11.025.
[27] C. Udhaya Kumar, A. Sethukumar, M. Velayutham Pillai, B. Arul Prakasam, C. Ramalingan, T. Vidhyasagar, Synthesis, spectral and structural studies of alkyl 2-(3-alkyl-2,6- diarylpiperidin-4-ylidene)hydrazinecarboxylate derivatives: crystal and molecular structure of methyl 2-(3-methyl-2,6- diphenylpiperidin-4-ylidene)hydrazinecarboxylate, J. Mol. Struct. 1112 (2016) 45–52. https://doi.org/10.1016/j.molstruc.2016.02.003.
[28] M.F. Hassan, A. Rauf, Synthesis and multi-spectroscopic DNA binding study of 1,3,4-oxadiazole and 1,3,4-thiadiazole derivatives of fatty acid, Spectrochim. Acta, Part A 153 (2016) 510–516. https://doi.org/10.1016/j.saa.2015.09.005.
[29] N. Shahabadi, S.M. Fili, F. Kheirdoosh, Study on the interaction of the drug mesalamine with calf thymus DNA using molecular docking and spectroscopic techniques, J. Photochem. Photobiol. B Biol. 128 (2013) 20–26. https://doi.org/10.1016/j.jphotobiol.2013.08.005.
[30] G. Zhang, P. Fu, L. Wang, M. Hu, Molecular spectroscopic studies of farrero interaction with calf thymus DNA, J. Agric. Food Chem. 59 (2011) 8944–8952. https://doi.org/10.1021/jf2019006.
[31] F. Ahmadi, A.A. Alizadeh, F.B. Saraskanrood, B. Jafari, M. Khodadadian, Experimental and computational approach to the rational monitoring of hydrogen bonding interaction of 2- imidazolidinethione with DNA and guanine, Food Chem. Toxicol. 48 (2010) 29–30. https://doi.org/10.1016/j.fct.2009.09.010.
[32] P. Kumar, S. Gorai, M.K. Santra, B. Mondal, D. Manna, DNA binding, nuclease activity and cytotoxicity studies of Cu (II) complexes of tridentate ligands, Dalton Trans. 41 (2012) 7573–7581. https://doi.org/10.1039/C2DT30232B.
[33] B.C. Baguley, M. LeBret, Quenching of DNA-ethidium fluorescence by amsacrine and other antitumor agents: a possible electron-transfer effect, Biochemistry 23 (1984) 937–943. https://doi.org/10.1021/bi00300a022.
[34] P.D. Ross, S. Subramanian, Thermodynamics of protein association reactions: forces contributing to stability, Biochemistry 20 (1981) 3096–3102. https://doi.org/10.1021/bi00514a017.
[35] A. Mukherjee, B. Singh, Binding interaction of pharmaceutical drug captopril with calf thymus DNA: a multispectroscopic and molecular docking study, J. Lumin. 190 (2017) 319–327. https://doi.org/10.1016/j.jlumin.2017.05.068.
[36] J.R. Lakowicz, Principle Fluor. Spect, third ed., Springer Publications, New York, 2006.
[37] R.A. Khan, A. SAsim, R. Kakkar, D. Gupta, V. Bagchi, F. Arjmand, S. Tabassum, A chloro-bridged heterobimetallic (η6-Arene) ruthenium–organotin complex as an efficient topoisomerase Iα inhibitor, Organometallics 32 (2013) 2546–2551. https://doi.org/10.1021/om301223k.
[38] P.D. Ross, S. Subramanian, Thermodynamics of protein association reactions: forces contributing to stability, Biochemistry 20 (1981) 3096–3102. https://doi.org/10.1021/bi00514a017.
[39] X. Guo, X. Li, Y. Jiang, L. Yi, Q. Wu, H. Chang, X. Diao, Y. Sun, X. Pan, N. Zhou, A spectroscopic study on the interaction between *p*-nitrophenol and bovine serum albumin, J. Lumin. 149 (2014) 353–360. https://doi.org/10.1016/j.jlumin.2014.01.036.
[40] D. Bhowmik, M. Hossain, F. Buzzetti, R. D'Auria, P. Lombardi, G.S. Kumar, Biophysical studies on the effect of the 13 position substitution of the anticancer alkaloid berberine on its DNA binding, J. Phys. Chem. B 116 (2012) 2314–2324. https://doi.org/10.1021/jp210072a.
[41] D. Sahoo, P. Bhattacharya, S.J. Chakravorti, Quest for mode of binding of 2-(4-(Dimethylamino)styryl)-1-methylpyridinium iodide with calf thymus DNA, Phys. Chem. B 114 (2010) 2044–2050. https://doi.org/10.1021/jp910766q.
[42] M.T. Carter, M. Rodriguez, A.J. Bard, Voltammetric studies of the interaction of metal chelates with DNA. 2. Tris-chelated complexes of cobalt(III) and iron(II) with 1,10-phenanthroline and 2,2'-bipyridine, J. Am. Chem. Soc. 111 (1989) 8901–8911. https://doi.org/10.1021/ja00183a029.
[43] T.R. Naik, S. Halehatty, B. Naik, M. Raghavendra, S.G.K. Naik, Synthesis of thieno[2,3-b]benzo[1,8]naphthyridine-2-carboxylic acids under microwave irradiation and interaction with DNA studies (06-2216LP), ARKIVOC xv (2006) 84–96. https://doi.org/10.3998/ark.5550190.0007.f11.
[44] C.V. Kumar, R.S. Turner, E.H.J. Asuncion, Groove binding of a styrylcyanine dye to the DNA double helix: the salt effect, Photochem. Photobiol. 74 (1993) 231–238. https://doi.org/10.1016/1010-6030(93)80121-O.
[45] Z. Seferoğlu, M.M.A. Mahmoud, H. Ihmels, Studies of the binding interactions of dicationic styrylimidazo[1,2-a]pyridinium dyes with duplex and quadruplex DNA, Dyes Pigments 125 (2016) 241–248. https://doi.org/10.1016/j.dyepig.2015.10.008.